IEEE Access
Multidisciplinary ⋮ Rapid Review ⋮ Open Access Journal

Received 1 September 2022, accepted 4 October 2022, date of publication 10 October 2022, date of current version 17 October 2022.

Digital Object Identifier 10.1109/ACCESS.2022.3213661

RESEARCH ARTICLE

Simultaneous Optimization of Mismatched Filters and Controlled Amplitude Signals for Long-Range MIMO Radars

PAVEL BEZOUŠEK AND SIMEON KARAMAZOV
Faculty of Electrical Engineering and Informatics, University of Pardubice, 53210 Pardubice, Czech Republic
Corresponding author: Simeon Karamazov (simeon.karamazov@upce.cz)

ABSTRACT This study presents a new signal and filter design procedure for long-range multiple-input multiple-output (MIMO) radars with a pulse length shorter than the return time of signals reflected by the most distant targets. The proposed algorithm adopts and radically improves the method of alternating the optimization of filters and signals, which was recently published by the same authors. It introduces full control of the signal envelope variation during the pulse, preserving acceptable peak-to-average power ratio (PAR) and signal-to-noise ratio (SNR) loss values. This state-of-the-art method allows calculation simplicity and is important for high-speed computations in adaptive applications. A gradient algorithm was used for the signal amplitude and phase optimization. The signal amplitude was controlled using a special signal construction consisting of two complex exponentials.

INDEX TERMS Crosstalk, Doppler effect, iterative optimization, gradient algorithm, MIMO radar, peak to average power ratio, quadratic programming, separation filter, side lobe, signal envelope, signal to noise ratio.

I. INTRODUCTION

MIMO communications and radar provide several advantages over conventional devices by significantly increasing the number of signal paths between the transmitter and the receiver. For example, in radars, this can be used to improve the detection parameters and space resolution. Given the same parameters, the transmitted power can then be used more efficiently, and the system can better adapt to different conditions and be protected against undesirable effects such as clutter or different types of interference. It is also possible to extend the functionality or accelerate the operation of the entire radar system by allowing a larger number of missions to be performed simultaneously. MIMO radar systems can be divided into two broad groups: collocated and distributed. In this paper, we discuss radars with collocated antennas, that is, antennas whose elements are spaced apart by fractions or multiples of a wavelength.

The associate editor coordinating the review of this manuscript and approving it for publication was Cheng Hu.

Many publications on MIMO radar have focused on signal optimization and compression/separation filters. Sophisticated MIMO signal and filter design methods have been developed and optimized, particularly for radars with pulses longer than the return time of the signal reflected from the farthest targets [1], [2], [3], [4], [5]. In addition, most of these methods deal only with constant envelope signals and matched filters. The matched filters allow for minimum loss and maximum use of the signal bandwidth for the radar range resolution. The constant envelope requirement is also understandable because it allows the transmission power to be optimized for the given transmitter parameters. These methods can achieve significant side-lobe and crosstalk suppression (100 dB or more), but only over a limited time lag. Some publications also deal with mismatched filters (e.g., [6], [7], and [8]), which, at the cost of a small increase in loss, allows improvements in side-lobe suppression and crosstalk over the entire time lag. If the constant envelope requirements are partially relaxed, it is possible to further improve the suppression of the side lobes and crosstalk over the entire lag by up to 20 dB (e.g., [9]).

The speed of the computation (optimization) of signals or filters is another aspect of the evaluation of design methods. Speed is of particular importance in systems where adaptive changes in operation are required, and it cannot be satisfied using a predefined set of signals and filters [10], [11], [12], [13], [14]. Most of the mentioned signal design algorithms are very complicated and computationally intensive; therefore, they do not meet these requirements. However, there are exceptions such as the algorithms in [10], [11], and [12].

Another issue is the optimization of signals and antennas in MIMO radar systems [12], [13], [14]. In particular, this concerns the optimization of antennas in collocated MIMO systems or station positions in distributed systems.

This paper presents an algorithm for optimizing filters and signals in collocated MIMO radar systems designed for target detection and tracking over long ranges. Such radars use pulsed signals with a length much shorter than the signal return time from the most distant targets. Typical examples of such radars are ground surveillance and approach or weather radar with maximum range of 150 – 450 km (return time is 1 – 3 ms) and pulse length of 10 – 300 μs. For these radars, efforts should be made to suppress all the side lobes and crosstalk.

This paper follows [9], where an SWAP algorithm is presented that splits the entire process into the optimization of individual filters and signals. Thus, the algorithm is relatively simple and computationally efficient, making it faster than variants of the WeCAN algorithm. Similarly, in [11], to speed up the WeCAN procedure [1], a conversion of the problem into an alternating optimization of individual signals was also used. However, the separation proposed in our previous paper is much more efficient and, unlike the aforementioned approach [11], allows the optimization of filters as well. The SWAP algorithm achieved significant suppression of side lobes and crosstalk as well as substantial simplification of calculations, thus speeding up the optimization. However, this comes at the cost of loosening the requirements for a constant signal envelope and maximum filter efficiency. In the vast majority of cases, the previous algorithm was able to design signals and filters with acceptable PAR and SNR loss values. However, in a limited number of cases, the unequal sizes of the elements of the complex envelope made this method unusable.

In this paper, we present an improved algorithm called UNISWAP that adopts the advantages of alternating filter and signal optimization while eliminating the main disadvantage of the previous algorithm, which is its inability to control the amplitude changes of the signals during the pulse and the SNR loss of the filters. The new algorithm allows either keeping of the envelope to be kept constant (equal to one) or accurately controls the signal amplitude variations during the pulse. The ratio of the maximum and minimum amplitudes of the signals can be set from one to infinity. Obviously, a small increase in loss (approximately 1 dB) and an increase in PAR (up to approximately 1.2) will not substantially degrade system performance. At the same time, the new algorithm allows significant improvements in the side lobe and crosstalk suppression.

As an optimization criterion, either integrated side-lobe level (ISL) or peak side-lobe (PSL) minimization can be chosen. For filter optimization, the new algorithm uses the least-squares (LS) method for the ISL criterion and quadratic convex programming for the PSL criterion [15], [16], [17], [18]. In contrast, for signal optimization, a gradient algorithm [19] was applied, as in [20]. However, in [20], only constant envelope signals and matched filters were assumed. To control the amplitude spread over a wider range, even with the gradient algorithm, a special signal construction is proposed that converts a problem with hard constraints into an unconstrained problem.

As shown by our testing, this algorithm can generate low PAR signals and low SNR loss filters with good suppression of side lobes and crosstalk under both the ISL and PSL criteria.

This paper is further organized as follows:

In Section 2, the notations of the quantities used and a mathematical description of the system are provided. Furthermore, the separation optimization method for each filter and signal is briefly described, along with the introduction of weights. Section 3 describes the gradient algorithm used for signal optimization. The method of optimizing the constant envelope signals and their extension to variable envelope signals is described. At the end of this section, the UNISWAP algorithm is summarized in tabular form. Section 4 presents the results of the testing of the proposed algorithm under various conditions. The optimization results (side-lobe and crosstalk suppression, PAR, and SNR loss), as well as the evolution of the minimized function throughout the optimization, are presented and discussed.

II. MATHEMATICAL DESCRIPTION

A. PROBLEM FORMULATION

A MIMO radar transmits M signals in pulses of length τ E and energy E. The mth signal complex envelope forms a vector

$$\mathbf{x}_m = \left[x_m(1), \ldots, x_m(i), \ldots, x_m(N)\right]^T, \quad m = 1, 2, \ldots, M, \tag{1}$$

with sampling period $T_S = \tau/N$. The energy of each signal is

$$E = \mathbf{x}_\mathbf{m}^H \cdot \mathbf{x}_m. \tag{2}$$

All signal complex envelopes can be assembled into a matrix

$$\mathbf{X} = \begin{bmatrix} x_1(1) & \cdots & x_M(1) \\ \vdots & & \vdots \\ \vdots & & \vdots \\ x_1(N) & \cdots & x_M(N) \end{bmatrix}. \tag{3}$$

At the receiving end, we use filters with coefficients $\mathbf{q}_m$ (4) to separate the signals by transmitters and compress the pulses

that concentrate the pulse energy on the main lobe.

$$\mathbf{q}_m = [q_m(1), \ldots, q_m(k), \ldots, q_m(K)]^T, \quad m = 1, 2, \ldots, M, \tag{4}$$

The coefficients meet the normalization condition

$$\mathbf{q}_m^{\mathrm{H}} \cdot \mathbf{x}_m = \mathbf{x}_{\mathbf{m}}^{\mathrm{H}} \cdot \mathbf{x}_m = \varepsilon. \tag{5}$$

Similar to the signals, the coefficients of the filters form a matrix

$$\mathbf{Q} = \begin{bmatrix} q_1(1) & \cdots & q_M(1) \\ \vdots & & \vdots \\ \vdots & & \vdots \\ q_1(K) & \cdots & q_M(K) \end{bmatrix}. \tag{6}$$

In our application, we consider *ed* $K = N$. The outputs of these filters are the convolutions of the signals and filter responses $\mathbf{z}_{m\mu} = \mathbf{x}_m * \mathbf{q}_\mu$. The elements of these convolutions, that is, the samples of signals at the outputs of the compression and separation filters, can be written as

$$z_{m\mu}(g) = \sum_{k=1}^{g+N} x_m(g + N + 1 - k) \, .q_\mu(k), \tag{7}$$

where the lag $g = 1 - N, \ldots, 0, \ldots, N - 1$. If $g > N$, the signal samples are $x_m(g) = 0$, if $k > N$, the filter coefficients are $q_\mu(k) = 0$.

From the convolution vectors, we construct the matrix

$$\mathbf{Z} = \begin{bmatrix} \mathbf{z}_{11} & \cdots & \mathbf{z}_{1\mu} & \cdots & \mathbf{z}_{1M} \\ \vdots & \ddots & \vdots & \ddots & \vdots \\ \mathbf{z}_{m1} & \cdots & \mathbf{z}_{m\mu} & \cdots & \mathbf{z}_{mM} \\ \vdots & \ddots & \vdots & \ddots & \vdots \\ \mathbf{z}_{M1} & \cdots & \mathbf{z}_{M\mu} & \cdots & \mathbf{z}_{MM} \end{bmatrix}_{M.(2N-1)\times M}. \tag{8}$$

The convolutions with $m = \mu$ represent the signal outputs of the corresponding filters. Ideally, these signals have the energy of the received pulse concentrated in the main lobe (sample with zero-time lag, $g = 0$), whereas the other samples (side lobes) should be minimal. Signals with $m \neq \mu$ indicate unwanted crosstalk that should be suppressed as much as possible. In this paper, we deal with the optimization of both the $\mathbf{x}_m$ signals and the $\mathbf{q}_\mu$ filters, with the goal of maximum suppression of sidelobes and crosstalk with minimum loss in the main lobes. Therefore, the requirement to minimize only the side lobes and crosstalk can be expressed as the requirement to minimize the norm.

$$\Phi = \|\mathbf{J} \odot \mathbf{Z}\|_\ell, \tag{9}$$

under condition (5), where

$$\mathbf{J} = \begin{bmatrix} \mathbf{j}_{11} & \cdots & \mathbf{j}_{1\mu} & \cdots & \mathbf{j}_{1M} \\ \vdots & \ddots & \vdots & \ddots & \vdots \\ \mathbf{j}_{m1} & \cdots & \mathbf{j}_{m\mu} & \cdots & \mathbf{j}_{mM} \\ \vdots & \ddots & \vdots & \ddots & \vdots \\ \mathbf{j}_{M1} & \cdots & \mathbf{j}_{M\mu} & \cdots & \mathbf{j}_{MM} \end{bmatrix}_{M.(2N-1)\times M} \tag{10}$$

$$\mathbf{j}_{m\mu} = \begin{bmatrix} j_{m\mu}(1 - N) \\ \vdots \\ j_{m\mu}(N - 1) \end{bmatrix},$$

$$j_{m\mu}(g) = \left(1 - \delta_{m\mu}\delta_{g0}\right) = j_{\mu m}(g). \tag{11}$$

The Kronecker symbol, $\delta_{m\mu} = 0$ for $m \neq \mu$ for $m = \mu$ is $\delta_{mm} = 1$ and $\odot$ is the symbol for the Hadamard product of matrices. Symbol ℓ represents the norm type. Clearly, if $\ell = F$ (Frobenius norm), the ISL criterion is used to minimize the expression Φ, and if $\ell = \infty$ (maximum norm), the PSL criterion is used.

B. SEPARATE OPTIMIZATION OF SIGNALS AND FILTERS

If we restrict ourselves to matched filters and constant envelope signals, the cyclic approximation (CA) methods described by several authors [1], [2], [3], [4], [20] can be used for optimization. Although remarkable results can be achieved by applying these methods, the suppression of side lobes and crosstalk is not significant, except in cases where suppression is favoured over a limited range of time lags g. Moreover, the aforementioned methods only apply the ISL criterion.

When we drop the requirements for matched filters but search for both optimal signals and suitable filters, much greater suppression can be achieved, and simultaneously, the optimization process is significantly accelerated. This procedure can be demonstrated using a matrix expression for the convolutions.

$$\mathbf{z}_{m\mu} = \mathbf{\Lambda}_m \cdot \mathbf{q}_\mu, \tag{12}$$

where $\mathbf{\Lambda}_m$ are Toeplitz matrices created of the signal vector $\mathbf{x}_m$

$$\mathbf{\Lambda_m}(\mathbf{x}_m) = \begin{bmatrix} x_m(1) & 0 & \ldots & 0 \\ x_m(2) & x_m(1) & \ddots & \vdots \\ \vdots & x_m(2) & \ddots & 0 \\ x_m(N) & \vdots & \ddots & x_m(1) \\ 0 & x_m(N) & \ddots & x_m(2) \\ \vdots & \ddots & \ddots & \vdots \\ 0 & \ldots & 0 & x_m(N) \end{bmatrix}. \tag{13}$$

For the minimized function Φ we get

$$\Phi = \|\mathbf{J} \odot (\mathbf{\Lambda} \cdot \boldsymbol{Q})\|_\ell, \tag{14}$$

where

$$\mathbf{\Lambda} = \begin{bmatrix} \mathbf{\Lambda_1} \\ \vdots \\ \mathbf{\Lambda_M} \end{bmatrix}. \tag{15}$$

Because neither the matrix $\mathbf{\Lambda}_m$ nor $\mathbf{J}$ depends on the coefficients of the filters, if we optimize only the filters $\mathbf{Q}$ at the given signals $\mathbf{X}$, the overall optimization can be separated into

the optimization of individual filters in parallel.

$$\mathbf{q}_\mu = \arg\left\{\min_{\mathbf{q}_\mu}\left[\Phi_\mu\right]\right\}, \quad \mu = 1, 2\ldots, M, \tag{16}$$

under condition (5), where

$$\Phi_\mu = \left\|\mathbf{J}_\mu \cdot \mathbf{\Lambda}\cdot\mathbf{q}_\mu\right\|_\ell, \quad \mathbf{J}_\mu = \mathbf{diag}\begin{bmatrix}\mathbf{j}_{1\mu}\\ \vdots \\ \mathbf{j}_{M\mu}\end{bmatrix}. \tag{17}$$

If we use the commutativity of the $\mathbf{z}_{m\mu}$ convolution, it can also be expressed as a matrix, as follows:

$$\mathbf{z}_{\mu m} = \mathbf{\Pi}_\mu\cdot\mathbf{x}_m, \tag{18}$$

$$\mathbf{\Pi}_\mu = \begin{bmatrix} q_\mu(1) & 0 & \ldots & 0 \\ q_\mu(2) & q_\mu(1) & \ddots & \vdots \\ \vdots & q_\mu(2) & \ddots & 0 \\ q_\mu(N) & \vdots & \ddots & q_\mu(1) \\ 0 & q_\mu(N) & \ddots & q_\mu(2) \\ \vdots & \ddots & \ddots & \vdots \\ 0 & \ldots & 0 & q_\mu(N) \end{bmatrix}. \tag{19}$$

Using the same procedure, we conclude that if we perform the minimization of Φ by optimizing the signals with specified filters, the task breaks down into separate optimizations of individual signals.

$$\mathbf{x}_m = \arg\left\{\min_{\mathbf{x}_m}\left[\Psi_m\right]\right\}; \quad m = 1, 2\ldots, M, \tag{20}$$

under condition (2), where

$$\Psi_m = \|\mathbf{J}_m \cdot \mathbf{\Pi}\cdot\mathbf{x}_m\|_\ell, \quad \Pi = \begin{bmatrix}\mathbf{\Pi}_1\\ \vdots \\ \mathbf{\Pi}_M\end{bmatrix}. \tag{21}$$

C. WEIGHTING OF SIDELOBES AND CROSSTALK

In some cases, assigning different weights to different side lobes and crosstalk during optimization are advantageous [1], [17], [20]. This can be achieved by modifying the diagonal matrices $\mathbf{J}_\mu$ (17). Taking a closer look at the elements of the main diagonal of these matrices, we find that, except for the main lobe corresponding to the signal-filter pair, all the elements are ones. By replacing the elements of the main diagonal of the matrix $\mathbf{J}_\mu$ with weights $w_{m,\mu}(g) \in \langle 0, 1\rangle$, we create weighting matrices $\mathbf{W}_\mu$ for the functions Φ_μ, while ensuring zeroing of the main lobes by setting $w_{mm}(0) = 0$. Usually, $w_{m,\mu}(g) = w_{\mu,m}(g)$, then we can use the same weighting matrices $\mathbf{W}_m$ for the functions Ψ_m. In the equations for the optimized functions Φ_μ, Ψ_m, instead of matrices $\mathbf{J}_\mu$, we insert weighting matrix $\mathbf{W}_\mu$

$$\Phi_\mu = \left\|\mathbf{W}_\mu\cdot\mathbf{\Lambda}\cdot\mathbf{q}_\mu\right\|_\ell, \quad \Psi_m = \|\mathbf{W}_m\cdot\mathbf{\Pi}\cdot\mathbf{x}_m\|_\ell, \tag{22}$$

$$\mathbf{W}_\mu = \mathbf{diag}\left[\mathbf{w}_{1,\mu}, \ldots, \mathbf{w}_{M,\mu}\right], \tag{23}$$

$$\mathbf{w}_{m,\mu} = \left[w_{m,\mu}(1-N), \ldots, w_{m,\mu}(N-1)\right], \tag{24}$$

Separate filter and signal optimizations can therefore be written in the form

$$\mathbf{q}_\mu = \arg\left\{\min_{\mathbf{q}_\mu}\left\|\mathbf{W}_\mu\cdot\mathbf{\Lambda}\cdot\mathbf{q}_\mu\right\|_\ell\right\}, \quad \mu = 1, 2\ldots, M, \tag{25}$$

under the condition

$$\mathbf{q}_m^{\mathrm{H}}\cdot\mathbf{x}_m = \mathbf{x}_\mathbf{m}^{\mathrm{H}}\cdot\mathbf{x}_m, \quad w_{m,m}(0) = 0, \tag{26}$$

and

$$\mathbf{x}_m = \arg\left\{\min_{\mathbf{x}_m}\|\mathbf{W}_m\cdot\mathbf{\Pi}\cdot\mathbf{x}_m\|_\ell\right\}; \quad m = 1, 2\ldots, M, \tag{27}$$

under the condition

$$\mathbf{x}_\mathbf{m}^{\mathrm{H}}\cdot\mathbf{x}_m = \varepsilon, \quad w_{m,m}(0) = 0. \tag{28}$$

Equations (25)–(28) allow the application of a cyclic algorithm alternating between filter and signal optimization.

If no requirements are placed on the signal amplitudes, an analytical solution (least-squares method) can be used for the Euclidean norm ($\ell = 2$), which significantly speeds up the iteration process. For the maximum norm ($\ell = \infty$), the problem can be solved using QPQC methods [16], [17], [18].

III. UNISWAP ALGORITHM

A. CONSTANT SIGNAL ENVELOPE

The above-mentioned approach achieved a significant improvement in side-lobe suppression (compared to the [1], [2], [3], [4], [5], and [20] algorithms) while maintaining acceptable values of PAR and SNR loss. However, the requirements for unit signal modulus and the use of matched filters must be relaxed.

In some cases, there was an excessive degradation of PAR and SNR loss; therefore, we began to search for a way to retain an efficient separation algorithm while having the envelope constant or maintaining its variations in a defined range (thus limiting the maximum magnitude of PAR).

First, we consider constant-envelope signals. Again, both steps of the algorithm alternately optimize filters to signals and signals to filters so that we preserve the most important feature of the SWAP algorithm. The filter optimization step can be implemented in the same manner according to (25) and (26), as in the case of the SWAP algorithm. In the signal optimization step, we must change condition (28), under which we perform minimization to

$$|x_m(n)| = 1 \Longleftrightarrow \mathbf{x}_m^* \odot \mathbf{x}_m = \mathbf{1}, \tag{29}$$

where, $\mathbf{1}$ is the column vector of N ones. Thus, the key step of the modified algorithm is to determine new signal vectors for the already computed filters under condition (29).

$$\mathbf{x}_m = \arg\left\{\min_{\substack{\mathbf{x}_m \\ \mathbf{x}_m^*\odot\mathbf{x}_m=1}}\left[\Psi_m\right]\right\}. \tag{30}$$

It is obvious that minimizing the expression Ψ_m will be the same as minimizing the function Ψ_m^2. Therefore, we can

remove the square root from the expression for the norm and use the weight matrix $\mathbf{W}_m$. Then, it can be written as:

$$\begin{aligned}\mathbf{x}_m &= \arg\left\{\min_{\substack{\mathbf{x}_m\\ \mathbf{x}_m^*\odot\mathbf{x}_m=\mathbf{1}}} \|\mathbf{W}_m\mathbf{\Pi}\mathbf{x}_m\|_\ell\right\}\\ &= \arg\left\{\min_{\substack{\mathbf{x}_m,\\ \mathbf{x}_m^*\odot\mathbf{x}_m=\mathbf{1}}} \Psi_m^2\right\}\\ &= \arg\left\{\min_{\substack{\mathbf{x}_m,\\ \mathbf{x}_m^*\odot\mathbf{x}_m=\mathbf{1}}} \|\mathbf{W}_m\mathbf{\Pi}\mathbf{x}_m\|_\ell^2\right\}. \end{aligned} \tag{31}$$

However, the normalization condition in (29) does not satisfy the requirements of the convex problem. Therefore, it is no longer possible to use a direct analytical solution for the ISL criterion or a solution according to [17] for the PSL criterion. Therefore, we used the classical gradient method [19] to minimize the function Ψ_m^2 using only the signal phases, as in [20]. The samples of the complex envelope, that is, the elements of vector $\mathbf{x}_m$ under the unit modulus requirement, can be expressed as

$$x_m(n) = e^{\mathrm{j}\varphi_m(n)}. \tag{32}$$

So, we will optimize N components of the phase vector

$$\boldsymbol{\varphi}_m = \begin{bmatrix}\varphi_m(1)\\ \vdots\\ \varphi_m(N)\end{bmatrix}. \tag{33}$$

The innovated phase vector ${}^{r+1}\boldsymbol{\varphi}_m$ is obtained by the rth iterative step of the gradient algorithm:

$${}^{r+1}\boldsymbol{\varphi}_m = {}^{r}\boldsymbol{\varphi}_m - {}^{r}\chi_m \cdot \nabla\Psi_m^2\left({}^{r}\boldsymbol{\varphi}_m\right). \tag{34}$$

where ${}^{r}\chi_m$ is the length of the rth iteration step and $\nabla\Psi_m^2\left({}^{r}\boldsymbol{\varphi}_m\right)$ is the gradient of the minimized function Ψ_m^2. When testing the algorithm, it was found that norm $\ell = 2$ was the best fit for the gradient algorithm, even in the case of the PSL criterion. Then we can write

$$\begin{aligned}\Psi_m^2 &= \|\mathbf{W}_m\mathbf{\Pi}\mathbf{x}_m\|_2^2 = \mathbf{x}_m^{\mathrm{H}}\mathbf{\Pi}^{\mathrm{H}}\mathbf{W}_m^{\mathrm{H}}\mathbf{W}_m\mathbf{\Pi}\mathbf{x}_m\\ &= \mathbf{x}_m^{\mathrm{H}}\mathbf{A}_m\mathbf{x}_m, \end{aligned} \tag{35}$$

where

$$\mathbf{A}_m = \mathbf{\Pi}^{\mathrm{H}}\mathbf{W}_m^{\mathrm{H}}\mathbf{W}_m\mathbf{\Pi}. \tag{36}$$

It is clear that matrix $\mathbf{A}_m$ is constant during the optimization of the signals because neither the weight matrix $\mathbf{W}_m$ nor the Toeplitz filter matrix $\mathbf{\Pi}$ depends on the signals. Thus, for the nth element of the gradient of the minimized function, the following holds.

$$\begin{aligned}\nabla_n\Psi_m^2\left(\boldsymbol{\varphi}_m\right) &\equiv \frac{\partial\Psi_m^2\left(\boldsymbol{\varphi}_m\right)}{\partial\varphi_m(n)}\\ &= \frac{\partial\mathbf{x}_m^{\mathrm{H}}}{\partial\varphi_m(n)}\mathbf{A}_m\mathbf{x}_m + \mathbf{x}_m^{\mathrm{H}}\mathbf{A}_m\frac{\partial\mathbf{x}_m}{\partial\varphi_m(n)}\\ &= 2\mathbf{Re}\left\{\mathbf{x}_m^{\mathrm{H}}\mathbf{A}_m\frac{\partial\mathbf{x}_m}{\partial\varphi_m(n)}\right\}. \end{aligned} \tag{37}$$

Because the partial derivatives of the signal vectors by phase are vectors containing all zeros except for one element,

$$\frac{\partial\mathbf{x}_m}{\partial\varphi_m(n)} = \left[0,\ldots,\mathrm{j}x_m(n),\ldots,0\right]^{\mathrm{T}}, \tag{38}$$

The calculation of the gradient was significantly simplified, and the entire iteration process was accelerated. The entire gradient can then be written in simple matrix form as

$$\nabla\Psi_m^2\left(\boldsymbol{\varphi}_m\right) = 2\mathbf{Re}\left\{\mathrm{j}\mathbf{x}_m\odot\left(\mathbf{x}_m^{\mathrm{H}}\mathbf{A}_m\right)^{\mathrm{T}}\right\}. \tag{39}$$

The gradient algorithm was terminated when the selected conditions, including the decrease in the minimized function and size of the gradient norm, were reached. The new value of the phase vector $\boldsymbol{\varphi}_m$ found by the described gradient algorithm becomes the innovated vector ${}^{i+1}\boldsymbol{\varphi}_m$ for the $i+1$-th step of the higher-level iteration of the UNISWAP algorithm. The new signal vector ${}^{i+1}\mathbf{x}_m$ is calculated according to equation (32).

B. CONTROLLED SIGNAL ENVELOPE

The UNISWAP algorithm maintains a constant envelope (PAR = 1), but the suppression of sidelobes and crosstalk is not as pronounced as when the SWAP algorithm is used, which does not limit the signal amplitudes. In Figs.1 and 2 filter outputs are presented for the system with M = 2 transmitted signals. The upper left and lower right subplots show filter responses to corresponding signals. Here we can see that using the SWAP algorithm with no control of signal amplitude variation the side lobe suppression reaches −60 dB but using UNISWAP with constant amplitude signals, the sidelobes are suppressed not so much. The same is true for crosstalk when filters are driven with not corresponding signals as shown on the upper right the lower left subplots. Thus, our goal was to regulate the possible spread of signal amplitudes to determine the optimal suppression of sidelobes and crosstalk at tolerable PAR values. Therefore, it was necessary to drop the constant amplitude condition (29), limiting the ratio of the maximum to minimum amplitude to a selected value of b.

$$\frac{\max\left(\mathbf{x}_m^*\odot\mathbf{x}_m\right)}{\min\left(\mathbf{x}_m^*\odot\mathbf{x}_m\right)} \le b. \tag{40}$$

These additional conditions in (40) are satisfied by the following signal construction:

$$\mathbf{x}_m = \exp\left(\mathrm{j}\boldsymbol{\varphi}\mathbf{0}_m\right) + a.\exp\left(\mathrm{j}\boldsymbol{\varphi}\mathbf{1}_m\right), \tag{41}$$

where

$$\boldsymbol{\varphi}\mathbf{0}_m = \begin{bmatrix}\varphi_m(1)\\ \vdots\\ \varphi_m(N)\end{bmatrix}, \quad \boldsymbol{\varphi}\mathbf{1}_m = \begin{bmatrix}\varphi_m(N+1)\\ \vdots\\ \varphi_m(2N)\end{bmatrix},$$
$$a = \frac{b-1}{b+1}. \tag{42}$$

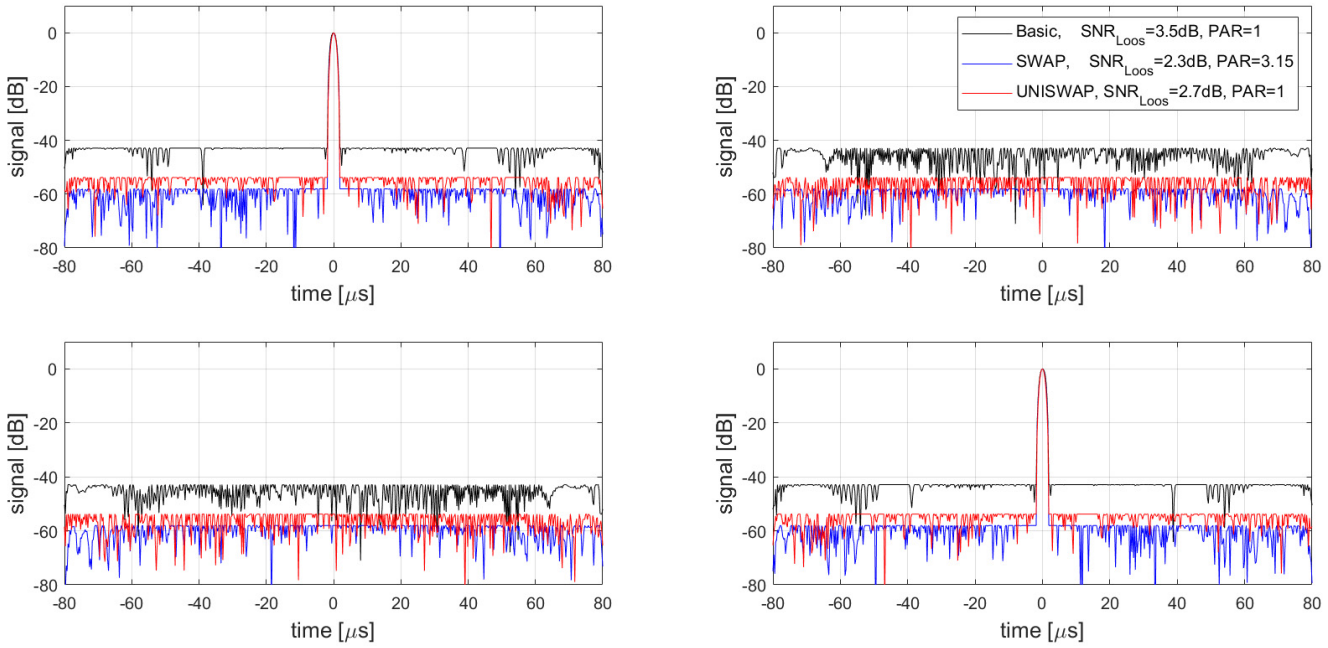

FIGURE 1. Comparison of side lobes and crosstalk suppression either by SWAP, UNISWAP (constant envelope), or just by optimized filters. Upper left and lower right graphs show the signals corresponding to filters – the main lobe and sidelobes, the rest plots show signals not corresponding to filters - crosstalk (PSL criterion $N = 300$, $M = 2$, $b = 1$).

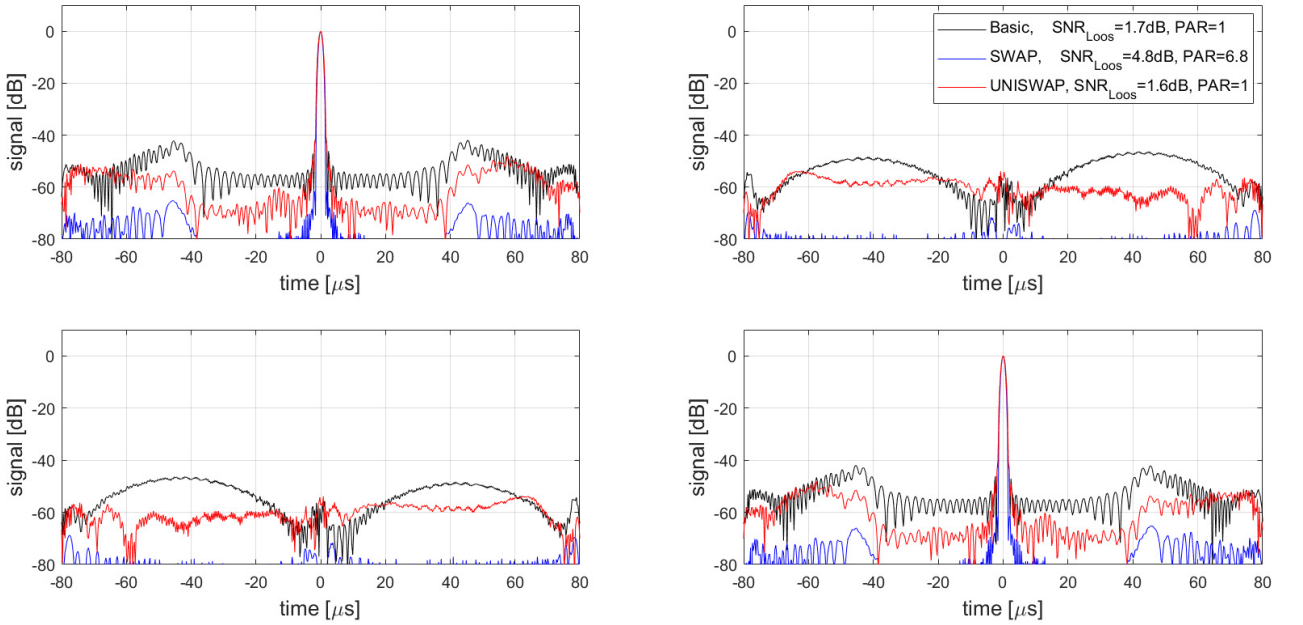

FIGURE 2. Comparison of side lobes and crosstalk suppression either by SWAP, UNISWAP (constant envelope), or just by optimized filters. Upper left and lower right graphs show the signals corresponding to filters – the main lobe and sidelobes, the rest plots show signals not corresponding to filters - crosstalk (ISL criterion, $N = 300$, $M = 2$, $b = 1$).

To simplify the notation, we merge the vectors $\boldsymbol{\varphi 0}_m$ and $\boldsymbol{\varphi 1}_m$ into the previously introduced phase vector $\boldsymbol{\varphi}_m$ expanded to $2N$ components:

$$\boldsymbol{\varphi}_m = \begin{bmatrix} \boldsymbol{\varphi 0}_m \\ \boldsymbol{\varphi 1}_m \end{bmatrix}. \tag{43}$$

By choosing the variables $\varphi_m(n)$, $n = 1, 2, \ldots, 2N$, in the interval $\langle 0, 2\pi \rangle$, for each sample of the mth signal, any sample phase in the interval $\langle 0, 2\pi \rangle$ and amplitude in the desired range can be set. We can then write the signal optimization as follows:

$$\begin{aligned} \boldsymbol{\varphi}_m &= \arg\left\{ \min_{\boldsymbol{\varphi}_m} [\Psi_m] \right\} \\ \mathbf{x}_m &= \exp\left(\mathrm{j}\boldsymbol{\varphi 0}_m\right) + a.\exp\left(\mathrm{j}\boldsymbol{\varphi 1}_m\right) \end{aligned} \tag{44}$$

For minimization, we used the same gradient method as in the algorithm for the constant envelope, but we now optimized the $2N$ components of the newly defined vector $\boldsymbol{\varphi}_m$.

To derive the gradient relation, we take advantage of the fact that the partial derivatives of the vectors $\mathbf{x}_m$ by the components of the vector $\boldsymbol{\varphi}_m$ are sparse vectors:

$$\frac{\partial \mathbf{x}_m}{\partial \varphi_m(n)} = \left[0, \ldots, \mathrm{j}\cdot \mathrm{e}^{\mathrm{j}\varphi_m(n)}, \ldots, 0\right]^{\mathrm{T}}, \quad \text{for } n = 1, 2, \ldots, N, \tag{45}$$

$$\frac{\partial \mathbf{x}_m}{\partial \varphi_m(n)} = a.\left[0, \ldots, \mathrm{e}^{\mathrm{j}\varphi_m(n)}, \ldots, 0\right]^{\mathrm{T}}, \quad \text{for } n = N+1, \ldots, 2N. \tag{46}$$

For the gradient, we then get the relation

$$\nabla \Psi_m^2(\boldsymbol{\varphi}_m) = 2\mathbf{Re}\left\{-\mathrm{j}\mathbf{x2}_m \odot \left(\mathbf{x2}_m^{\mathrm{H}}\mathbf{A}_m\right)^{\mathrm{T}}\right\}, \tag{47}$$

where $\mathbf{x2}_m$ is a column vector with $2N$ components.

$$\mathbf{x2}_m = \begin{bmatrix} \mathrm{e}^{\mathrm{j}\varphi_m(1)} \\ \vdots \\ \mathrm{e}^{\mathrm{j}\varphi_m(N)} \\ a.\mathrm{e}^{\mathrm{j}\varphi_m(N+1)} \\ \vdots \\ a.\mathrm{e}^{\mathrm{j}\varphi_m(2N)} \end{bmatrix}. \tag{48}$$

Then the signal vectors $\mathbf{x}_m$ we get using (44).

C. ALGORITHM DESCRIPTION

The entire UNISWAP optimization algorithm is summarized in the procedure described in TABLE 1. The individual steps of the SWAP iterations are denoted by superscript i.

TABLE 1. The UNISWAP algorithm.

Step 0: Create an initial unimodular signal set ${}^0\mathbf{x}_m$ and calculate the respective phase set ${}^0\boldsymbol{\varphi}_m$,
Step 1: Build matrices $\mathbf{W}_\mu$ and $\boldsymbol{\Lambda}$ from vectors ${}^i\mathbf{x}_m$
Step 2: Calculate filters ${}^i\mathbf{q}_\mu$ using ISL or PSL criterium
Step 3: Build matrices $\boldsymbol{\Pi}_m$ and $\boldsymbol{\Pi}$ from the filters ${}^i\mathbf{q}_\mu$
Step 4: Calculate a new phase vector ${}^{i+1}\boldsymbol{\varphi}_m$ using the gradient algorithm and the respective signal set ${}^{i+1}\mathbf{x}_m$
Step 5: Repeat Steps 2–4 until the criterion selected for the UNISWAP algorithm is achieved.

The calculation of filters in step 2 based on the ISL or PSL criteria is described in [9]. The gradient algorithm in Step 4 is a standard algorithm that searches for optimal signals for the given filters using an iterative method. To compute the gradient in the case of $\ell = 2$, a computationally efficient analytical method was used (see relations (39) and (47)). For $\ell = \infty$, a numerical calculation should be used. However, owing to the aforementioned advantage of using the Euclidean metric in the gradient algorithm, this approach was not used in the UNISWAP algorithm.

IV. ALGORITHM EXAMINATION

The structure of the UNISWAP algorithm is based on the commutativity of convolution. This alternates between finding the optimal filters for the initial signals, and finding a new signals for the determined filters. These two successive computations are called one swap, where the order of the swaps is denoted by the variable i. In the previously published simpler SWAP algorithm, the optimization methods used for filters and signals are the same, corresponding to the chosen criterion; in the new UNISWAP algorithm, the computation of the new signals is performed using a gradient method. Although these calculations are more complex and somewhat longer, they eliminate the main disadvantage of the previous algorithm, which is the impossibility of controlling the signal envelope changes through the pulse. The gradient algorithm not only maintains the envelope constant but also controls the ratio between the maximum and minimum sizes of the elements of the signal vector. At each ith swap of the UNISWAP algorithm, another iterative process of the gradient algorithm was executed with steps denoted by r. In each step of the gradient algorithm, a line search method was applied to determine the appropriate step length using the Armijo rule [21].

To demonstrate the algorithm, we chose the initial signals with linear frequency modulation. The time-bandwidth product of this signal is $B\tau = 100$, where B is the instantaneous signal bandwidth and τ is the pulse length. Signals with such characteristics are typically used in medium-to long-range ground-based surveillance radar because of their low sensitivity to the Doppler effect. These signals are frequency-diversified (FD) in MIMO radar applications.

A. COMPARISON OF SWAP AND UNISWAP ALGORITHMS

The constant envelope of the signals (parameter $b = 1$, i.e., $a = 0$) implies a significant tightening of the requirements for signal optimization compared to the original SWAP algorithm. This results in the deterioration of side-lobe suppression compared to the original algorithm. Figs. 1 and 2 present a comparison of side-lobe suppression and crosstalk between the results of the UNISWAP algorithm at a constant signal amplitude (PAR = 1) and the original SWAP algorithm without amplitude constraints. Both cases used PSL and ISL criteria. In the sample figures, we see that the suppression in the constant envelope case (red curves) is slightly greater than the initial values before the application of the algorithm (black curves), but worse than when using the SWAP algorithm (blue curves). A larger optimization effect (up to 7 dB) was observed for the ISL, mainly for the nearer side lobes. In the case of PSL, the improvement over baseline did not depend on the time lag; however, it was only 4 dB.

In practice, a slight increase in the PAR of the transmitted signal does not imply a large degradation of the transmitter characteristics or a significant distortion of the signal.

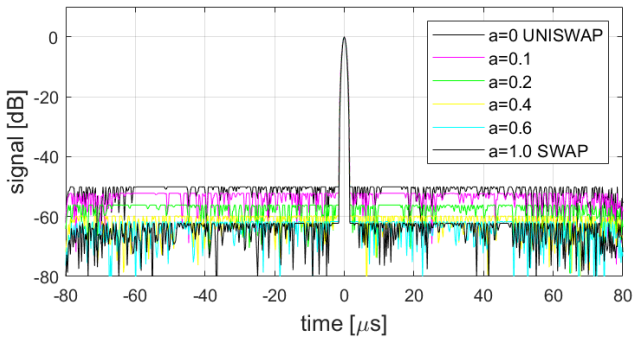

FIGURE 3. Comparison of algorithm results for PSL criterion. It is clearly seen how for different values of parameter *a*, the curve levels are between the SWAP (arbitrary signal amplitude) and UNISWAP (unit signal amplitude).

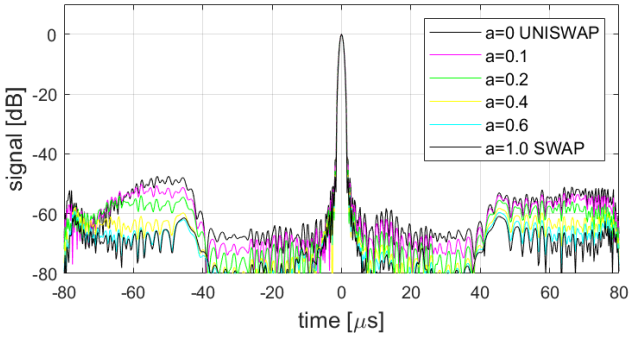

FIGURE 4. Comparison of algorithm results for ISL criterion. For different values of parameter *a*, the curves are again in positions between SWAP (arbitrary signal amplitude) and UNISWAP (unit signal amplitude) levels.

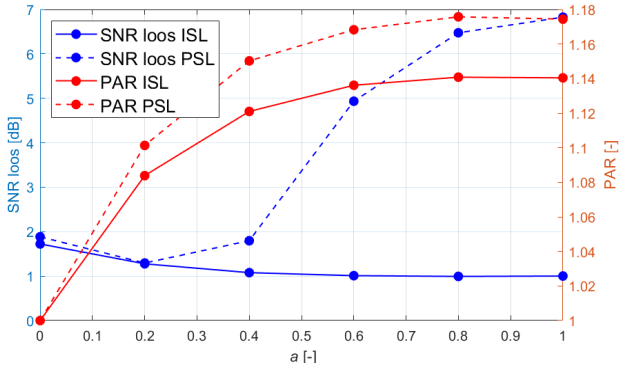

FIGURE 5. Dependence of SNR loss and PAR for ISL and PSL criterion on the optimization parameter *a*, limiting the signal amplitude spread.

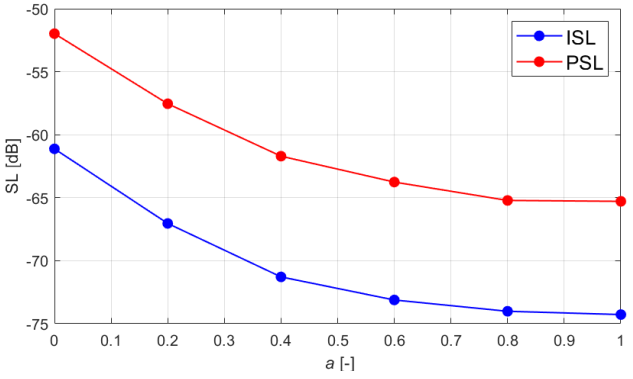

FIGURE 6. Dependence of side lobe suppression (SL) on the parameter *a* for both ISL and PSL criteria.

However, even a small relaxation of the constant envelope requirement allows for a further increase in the side lobe and crosstalk suppression. The results are shown in Figs. 3 and 4. Here, the waveforms of the signals emerging from the separation filters optimized by the UNISWAP algorithm are plotted for several values of the parameter $a = 0$ to 1. As this parameter increases from $a = 0$ (constant envelope signal) to $a = 1$ (signal amplitude variations are not constrained at all), the suppression of the side lobes and crosstalk gradually improves until it approaches the results obtained using the SWAP algorithm.

At the same time However, the PAR of the transmitted signal increases slightly from PAR = 1 to PAR < 1.2, as shown in Fig. 5. We observed that this deterioration is very low for both the ISL and PSL criteria. However, we observed different behaviors in the SNR loss parameters. With the ISL criterion, the loss decreases steadily with the increase in parameter a. For the PSL criterion, it reaches a minimum at $a = 0.2$, and then increases sharply to values of approximately 6 dB. This is in contrast with our previous findings [9]. With the SWAP algorithm the PAR for the ISL criterion deteriorates significantly, and on the other hand, the losses stay below 2 dB in all cases. Hence, it can be concluded that the SWAP and UNISWAP algorithms at $a = 1$ are not identical, but each converges to a different minimum. However, UNISWAP provides very good results in terms of side-lobe suppression as well as in PAR parameter values (Fig. 6). Excellent results were obtained for SNR loss when the ISL criterion was chosen. The side-lobe suppression changes mostly between $a = 0$ and 0.4 (Fig. 6), beyond which the improvement is insignificant, whereas the PAR value still increases slightly. Therefore, the choice of $a = 0.4$ to 0.5 may be appropriate.

B. DOPPLER SHIFT EFFECT ON SIDE LOBES AND CROSSTALK SUPPRESSION

The Doppler effect can be included in the optimization of signals and filters by extending the minimized function to include signals with selected Doppler shifts f_d [9], [20]. The degree of influence of the Doppler effect on the signals can be estimated from the magnitude of the signal phase change $\Delta\phi_{\max}$ due to the Doppler shift along the entire pulse:

$$\Delta\phi_{\max} = 2\pi f_\mathrm{d}\tau. \tag{49}$$

If the phase change is $\Delta\phi_{\max} \ll 2\pi$, then this effect is usually insignificant. For example, ground-based surveillance radars (GBSR) for air traffic control (ATC) deal with targets moving maximally at the speed of sound, and the Doppler shift of the frequency is limited to $f_\mathrm{d} < 6$ kHz. The maximum phase change is then $\Delta\phi_{\max} < 1.2\pi$. This is probably at

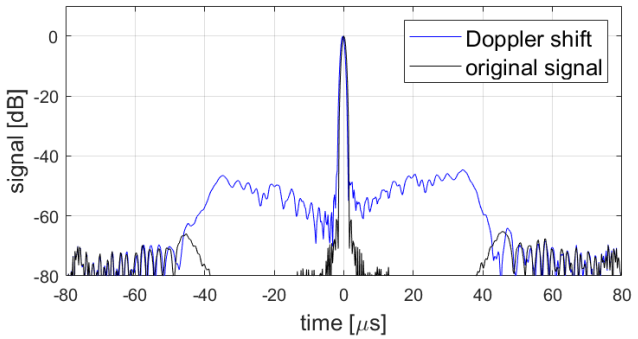

FIGURE 7. Comparison of the original signal and signal with doppler shift f_d = 5kHz for ISL optimization.

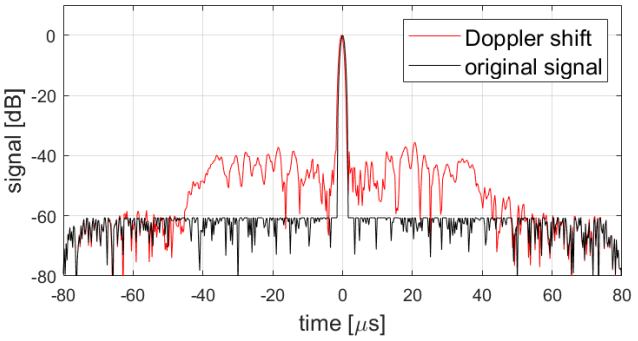

FIGURE 8. Comparison of the original signal and signal with doppler shift f_d = 5kHz for PSL optimization.

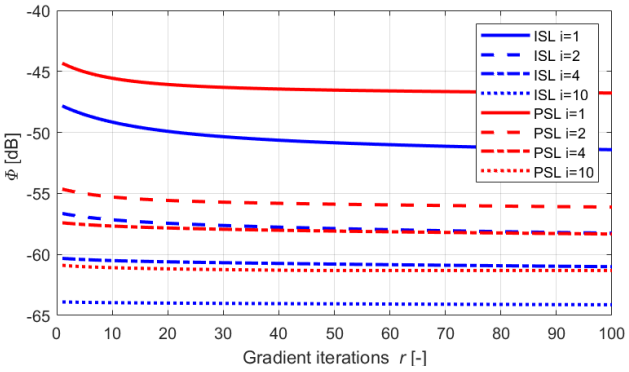

FIGURE 9. Dependence of the minimized function Φ on the number of steps r at a given step i of the UNISWAP algorithm.

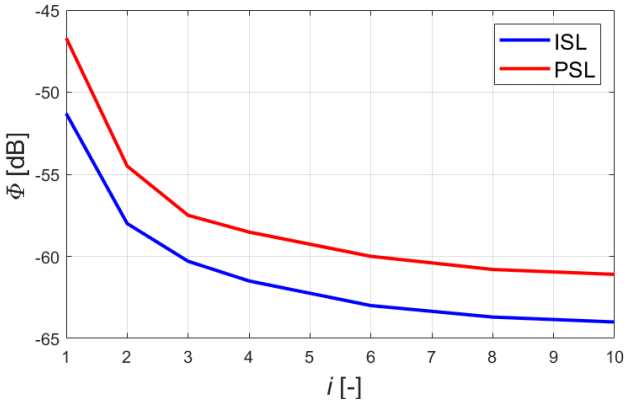

FIGURE 10. Dependence of the value of the minimized function Φ on iteration step i of the UNISWAP algorithm.

the edge of a situation where this influence can be neglected. Figures 7 and 8 show the amplitudes of the output signals when the received signals are affected by a Doppler shift of 5 kHz.

In this case, without including the Doppler effect in the optimization, the side-lobe suppression (similar to crosstalk) is degraded by up to 25 dB; however, the suppression remains higher than 30 dB. If we include the influence of the Doppler effect in the optimization, the deterioration is reduced; however, there is some deterioration for all Doppler shifts, including the zero shift. It should be noted that the greatest suppression of side lobes and crosstalk should be achieved for targets with large radar cross-sections (RCS), that is, targets that are static or moving at lower velocities. Thus, the result of including the Doppler effect at high velocities in the optimization is questionable.

C. EFFECT OF PARAMETER CHOICE ON CONVERGENCE AND RESULTS OF THE UNISWAP ALGORITHM

Several parameters that affect the convergence and optimization results can be selected for the algorithm under study. The first is the ISL or PSL criterion. Both criteria were used to optimize the filters. For signal optimization, this can also be implemented by choosing the order ℓ of the norm. The ISL corresponds to $\ell = 2$ and the PSL corresponds to $\ell = \infty$. However, experiments with the gradient algorithm have shown that the efficiency of this algorithm for $\ell > 2$ decreases rapidly as ℓ increases and that for $\ell = \infty$ it is completely inefficient. Therefore, in the gradient algorithm, we used only the norm $\ell = 2$. The use of the ISL or PSL criterion for the filters provides standard suppression properties, as shown in Figs. 3 and 4. With ISL, higher suppression of the near side lobes ($|g| \leq N/2$) was achieved, while the far-side lobes ($|g| \approx N$) remained quite high. With the PSL criterion, the suppression of all lateral lobes and crosstalk is the same (unless the same weights are used), but only moderate. However, the ISL algorithm was significantly faster than the PSL criteria.

The effect of parameter a, which limits the spread of the signal amplitudes during the pulse, on the results was discussed in the previous section. However, this parameter also affects the convergence speed. As the value of a increases, the computational effort increases, which makes the computation longer.

Figure 9 plots the values of the minimized function Φ^2 at the end of each step r of the gradient algorithm at the given step i of the UNISWAP algorithm.

$$\Phi^2 = \sum_{m=1}^{M} \Psi_m^2 = \sum_{\mu=1}^{M} \Phi_\mu^2, \tag{50}$$

where

$$\Phi_\mu = \left\| \mathbf{W}_\mu \cdot \mathbf{\Lambda} \cdot \mathbf{q}_\mu \right\|_\ell , \quad \Psi_m = \| \mathbf{W}_m \cdot \mathbf{\Pi} \cdot \mathbf{x}_m \|_\ell . \quad (51)$$

We can see that, for both criteria (ISL and PSL), the minimized function Φ decreases smoothly with both increasing r and increasing i. Understandably, the decrease is always more significant in the first steps than in the later steps. The graph shows that the first 30–50 steps are the most significant. When optimizing the filters within the UNISWAP algorithm, there is always a decrease in the function Φ. This improvement was significant only at lower values of i. In Fig. 10, it can be observed that the difference between the values of the minimized function for $i = 8$ and $i = 10$ for both criteria is only approximately 0.5 dB. These findings allowed for a reduction in the maximum number of steps.

V. CONCLUSION

In this paper, an algorithm called UNISWAP is presented for the optimization of signals and filters in MIMO radars with the goal of maximum suppression of time-side lobes and crosstalk over the entire lag. It is based on alternating filter and signal optimization, allowing the separation of each iteration step into parallel optimizations of individual filters or signals. This significantly reduces computational effort and accelerates the entire procedure. Compared to the classic WeCAN algorithm, our UNISWAP algorithm is up to a hundred times faster in the case of the ISL criterion (analytical calculation) and roughly thirty times faster in the case of the PSL criterion (numerical calculation) on the same hardware. In contrast to the previously published SWAP algorithm, which is based on the same idea, the new algorithm enables control of signal amplitude variations during the pulse. It is exploited to improve the suppression of side lobes and crosstalk by as much as 7 dB while preserving low PAR under 1.2 and SNR loss less than 1 dB. The effect of Doppler shift was also assumed. It is shown that even if the radial target velocity reaches the speed of sound, the side lobe and crosstalk suppression do not fall below –30 dB, which seems to be sufficient in most applications.

REFERENCES

[1] H. He, P. Stoica, and J. Li, "Designing unimodular sequence sets with good correlations—Including an application to MIMO radar," *IEEE Trans. Signal Process.*, vol. 57, no. 11, pp. 4391–4405, Nov. 2009.
[2] S. Ahmed and M.-S. Alouini, "MIMO-radar waveform covariance matrix for high SINR and low side-lobe levels," *IEEE Trans. Signal Process.*, vol. 62, no. 8, pp. 2056–2065, Apr. 2014.
[3] Z. Zhou, S. Zhao, Q. Shi, and R. Zhang, "Sequence set design with min-max criterion using majorization-minimization," in *Proc. IEEE/CIC Int. Conf. Commun. China (ICCC)*, Aug. 2019, pp. 550–555.
[4] J. Song, P. Babu, and D. P. Palomar, "Sequence set design with good correlation properties via majorization-minimization," *IEEE Trans. Signal Process.*, vol. 64, no. 11, pp. 2866–2879, Jun. 2016.
[5] A. Bose, I. A. Arriaga-Trejo, A. G. Orozco-Lugo, and M. Soltanalian, "Generalized cyclic algorithms for designing unimodular sequence sets with good (complementary) correlation properties," in *Proc. IEEE 10th Sensor Array Multichannel Signal Process. Workshop (SAM)*, Jul. 2018, pp. 287–291.
[6] C. Y. Chen and P. P. Vaidyanathan, "MIMO radar waveform optimization with prior information of the extended target and clutter," *IEEE Trans. Signal Process.*, vol. 57, no. 9, pp. 3533–3544, Sep. 2009.
[7] L. Xu, H. Liu, S. Zhou, H. Ma, J. Zheng, and J. Wang, "Joint optimization of transmit waveform and mismatched filter with expanded main lobe for delay-Doppler side lobes suppression," in *Proc. Int. Conf. Radar (RADAR)*, Brisbane, QLD, Australia, Aug. 2021, pp. 1–6.
[8] G. Cui, H. Li, and M. Rangaswamy, "MIMO radar waveform design with constant modulus and similarity constraints," *IEEE Trans. Signal Process.*, vol. 62, no. 2, pp. 343–353, Jan. 2014.
[9] P. Bezousek and S. Karamazov, "Joint optimization of signal waveforms and filters for long-range MIMO radars," *IEEE Access*, vol. 10, pp. 33238–33247, 2022, doi: 10.1109/ACCESS.2022.3161731.
[10] Y. Yu, Z. Junhui, and L. Wu, "Adaptive waveform design for MIMO radar-communication transceiver," *Sensors*, vol. 18, pp. 1–16, Jun. 1957.
[11] J. Zhang, N. Xu, H. Song, and C. Zhang, "Sequence set design for waveform-agile coherent radar systems," *EURASIP J. Adv. Signal Process.*, vol. 2020, no. 1, pp. 1–17, Dec. 2020, doi: 10.1186/s13634-020-00689-0.
[12] M. Bolhasani, S. Imani, and S. A. Ghorashi, "A simple and fast method to generate transmit beampattern in MIMO radar," *Int. J. Innov. Res. Elect., Electron., Instrum. Control Eng.*, vol. 3, no. 8, pp. 77–82, Aug. 2015.
[13] M. Chakraborty, D. Bhaskar, R. Bera, and S. Sarkar, "Designing a MIMO digital MVDR beam former using STAP processing for adaptive steering of antenna beam," *Int. J. Mobile Commun. Netw.*, vol. 2, no. 1, pp. 51–56, 2011.
[14] K. Shadi and F. Behnia, "Transmit beampattern synthesis using eigenvalue decomposition in MIMO radar," in *Proc. 8th Int. Conf. Inf., Commun. Signal Process.*, Singapore, Dec. 2011, pp. 1–10, doi: 10.1109/ICICS.2011.6174302.
[15] S. Boyd and L. Vandenberghe, *Convex Optimization*, 7th ed. Cambridge, U.K.: Cambridge Univ. Press, 2009, p. 730.
[16] O. Rabaste and L. Savy, "Mismatched filter optimization via quadratic convex programming for radar applications," in *Proc. Int. Radar Conf.*, Lille, France, Oct. 2014, pp. 1–5.
[17] O. Rabaste and L. Savy, "Quadratically constrained quadrature programs for mismatched filter optimization with radar applications," Centre pour la Commun. Scientifique Directe, France, Working Paper hal-01080572, 2014. [Online]. Available: https://hal.archives-ouvertes.fr/hal-01080572
[18] P. Bezousek, S. Karamazov, and J. Rolecek, "Adaptive pulse compression filter in radar receiver application," in *Proc. Conf. Microw. Techn. (COMITE)*, Pardubice, Czech Republic, Apr. 2019, p. 4.
[19] E. K. P. Chong and S. H. Zak, "Gradient methods," in *An Introduction to Optimization*, 4th ed. Hoboken, NJ, USA: Wiley, 2013, ch. 8, pp. 131–160.
[20] F. Wang, C. Pang, Y. Li, and X. Wang, "Designing constant modulus sequences with good correlation and Doppler properties for simultaneous polarimetric radar," *Electronics*, vol. 7, no. 8, p. 153, Aug. 2018.
[21] W. Sun and X. Y. Yuan, *Optimization Theory and Methods: Nonlinear Programming*. New York, NY, USA: Springer, 2006, pp. 103–104.

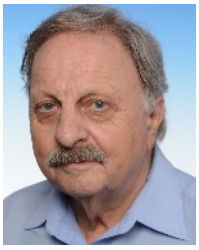

PAVEL BEZOUŠEK was born in Ostrava, Czechoslovakia, in 1943. He received the M.S. and Ph.D. degrees from Czech Technical University in Prague, in 1966 and 1980, respectively. He worked with the Radio Research Institute of Tesla Pardubice, from 1966 to 1994, where he was engaged in microwave circuit and system design. Since then, he has been with the University of Pardubice, currently he is with the Faculty of Electrical Engineering and Informatics, as a Full Professor in radar system design.

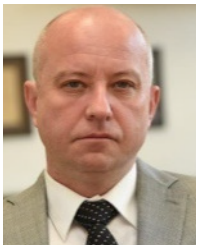

SIMEON KARAMAZOV was born in Pardubice, Czechoslovakia, in 1963. He received the Ing. degree from Czech Technical University in Prague, in 1987, and the Dr. degree from the University of Pardubice, in 1994, where he is currently pursuing the Ph.D. degree in solid-state physics and semiconductors. Since 1991, he has been working at the University of Pardubice, currently he is with the Department of Mathematics and Physics, Faculty of Electrical Engineering and Informatics, as a Full Professor.